Supporting Information

Chromogenic naked-eye detection of copper ion and fluoride

Ye Won Choi, Jae Jun Lee, Ga Rim You, Sun Young Lee, Cheal Kim*

Department of Fine Chemistry and Department of Interdisciplinary Bio IT Materials, Seoul National University of Science and Technology, Seoul 139-743, Korea. Fax: +82-2-973-9149; Tel: +82-2-970-6693; E-mail:chealkim@seoultech.ac.kr

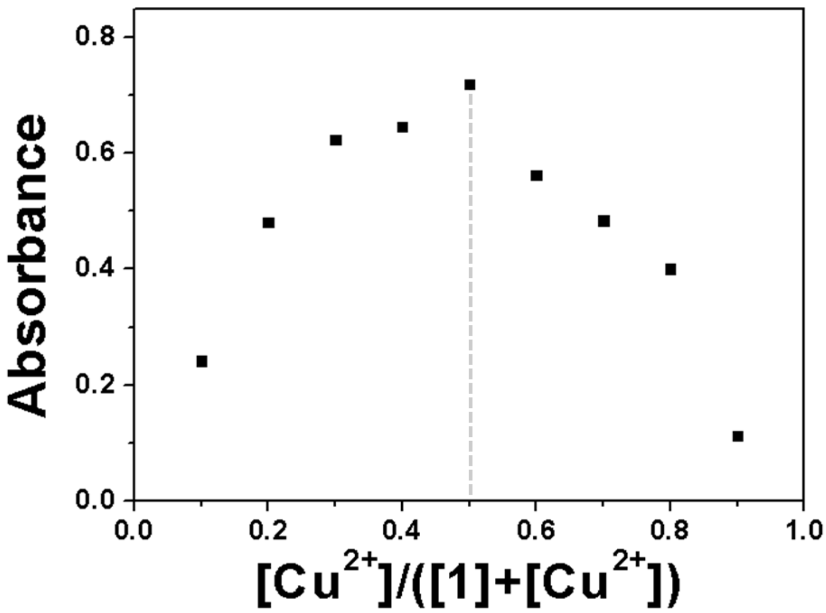

Fig. S1 Job plot of **1** and Cu^{2+}. The total concentrations of **1** and Cu^{2+} were 100 μM.

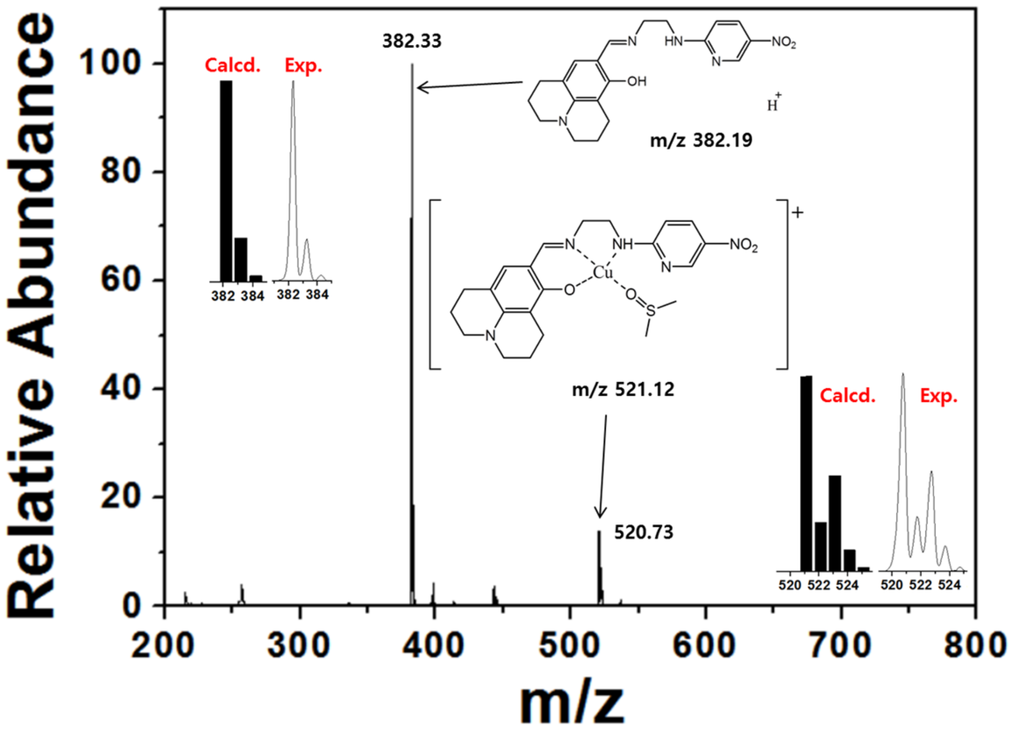

Fig. S2 Positive-ion electrospray ionization mass spectrum of **1** (100 μM) upon addition of 1 equiv of $Cu(NO_3)_2$.

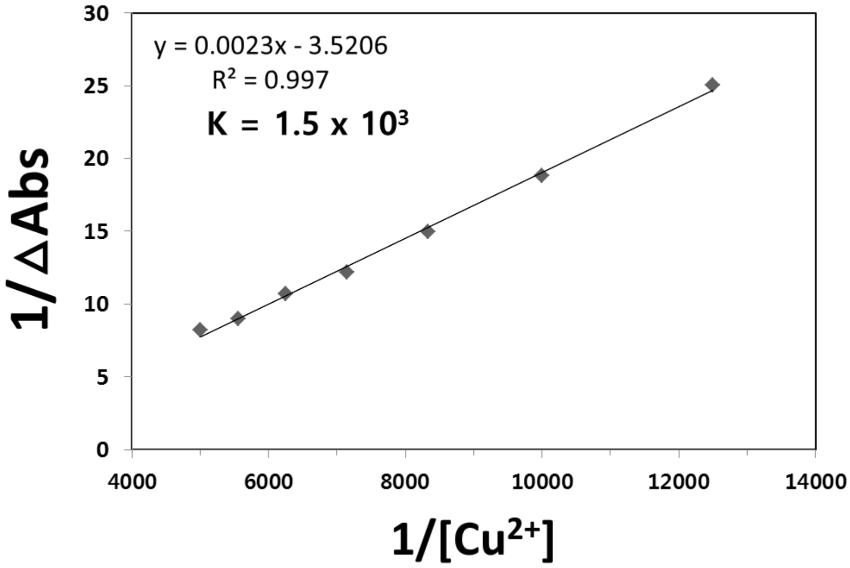

Fig. S3 Benesi-Hildebrand plot of **1** (at 450 nm), assuming 1:1 stoichiometry for association between **1** and Cu^{2+}.

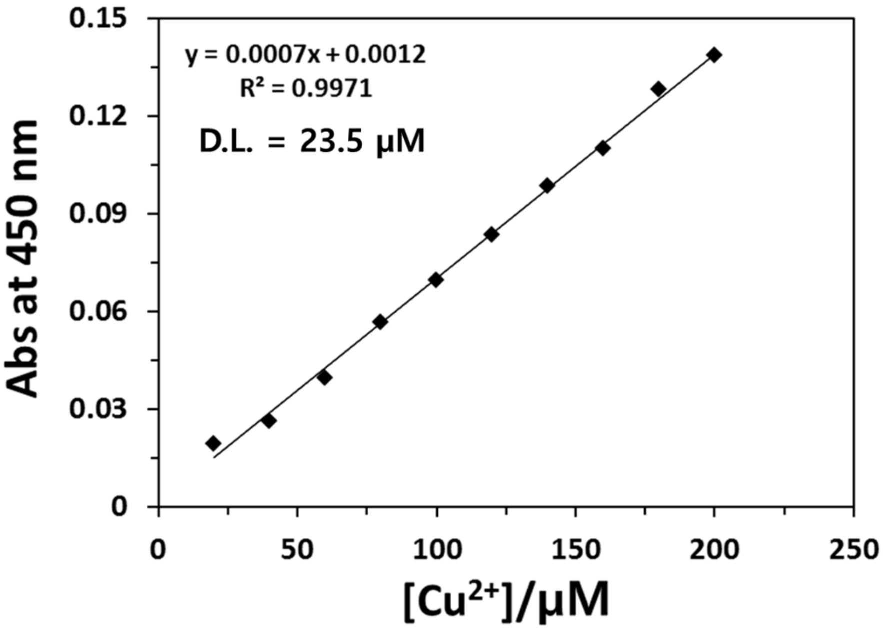

Fig. S4 Detection limit of **1** (20 μM) for Cu^{2+} through change of absorbance at 450 nm.

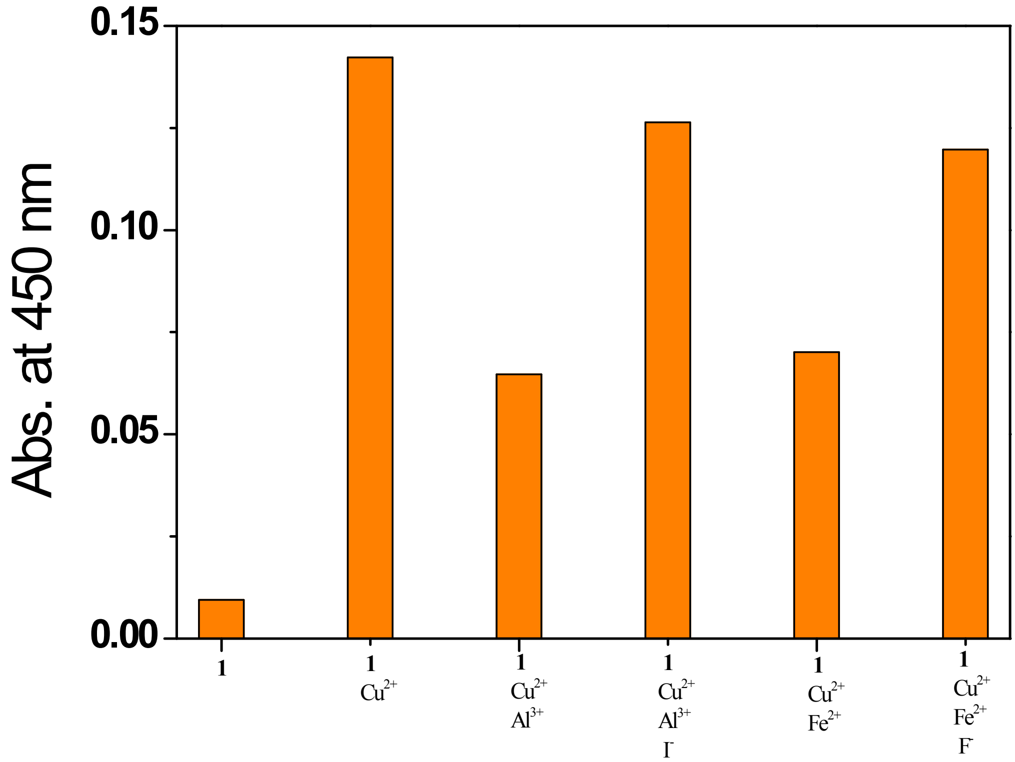

Fig. S5 Recovery tests of **1**-Cu^{2+}-Al^{3+} in presence of I^- and **1**-Cu^{2+}- Fe^{2+} in presence of F^- in acetonitrile-water (7:3, v/v).

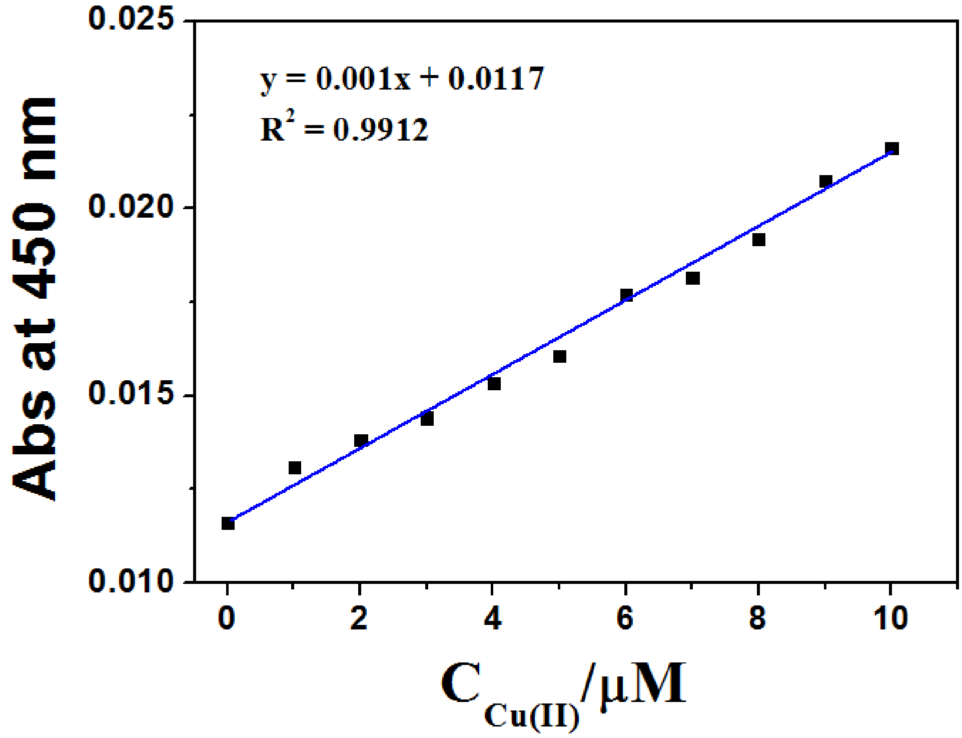

Fig. S6 Absorbance (at 450 nm) of **1** as a function of Cu^{2+} concentration ([**1**] = 20 μmol/L and [Cu^{2+}] = 0 - 10 μmol/L).

(a)

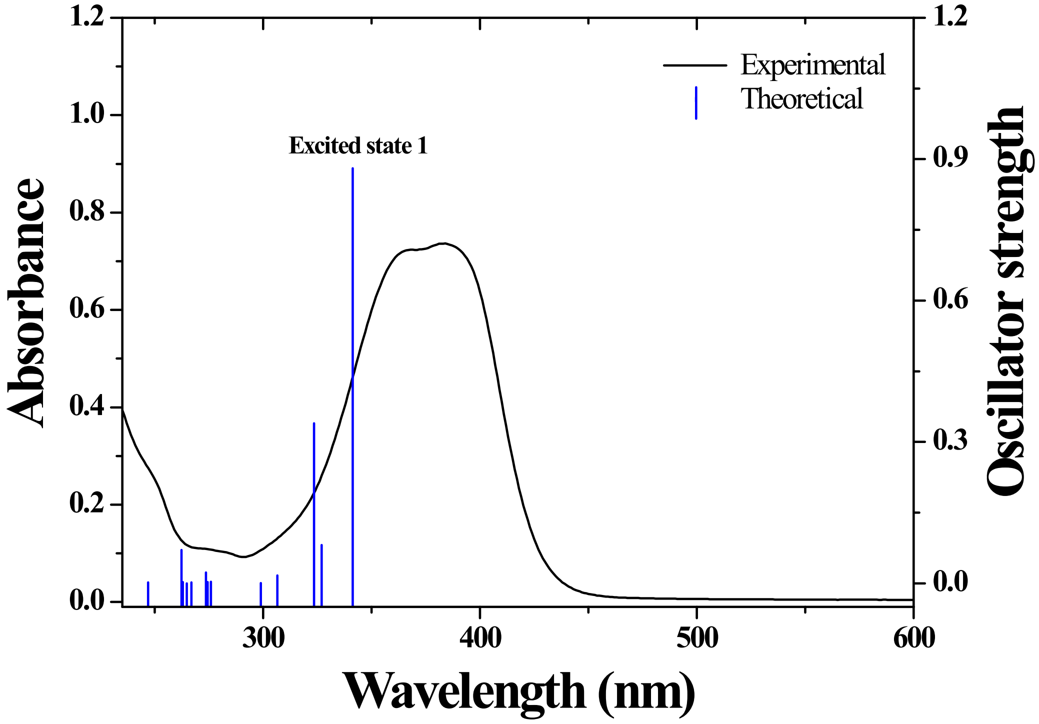

(b)

Excited State 1	Wavelength	Percent (%)	Main character	Oscillator strength
H-2 → L	341.34 nm	79 %	ICT	0.8808
H → L+1		20 %	ICT	

(c)

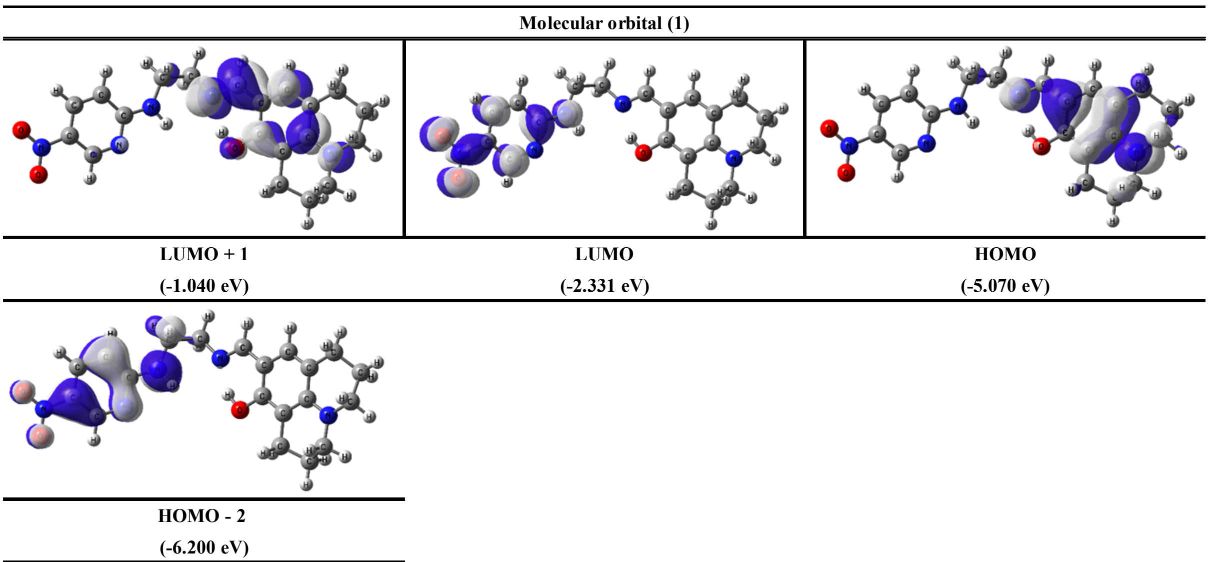

Fig. S7 (a) The theoretical excitation energies and the experimental UV-vis spectrum of **1**. (b) The major electronic transition energies and molecular orbital contributions for **1** (H = HOMO and L = LUMO). (c) Isosurface (0.030 electron bohr^{-3}) of molecular orbitals participating in the major singlet excited states of **1**.

(a)

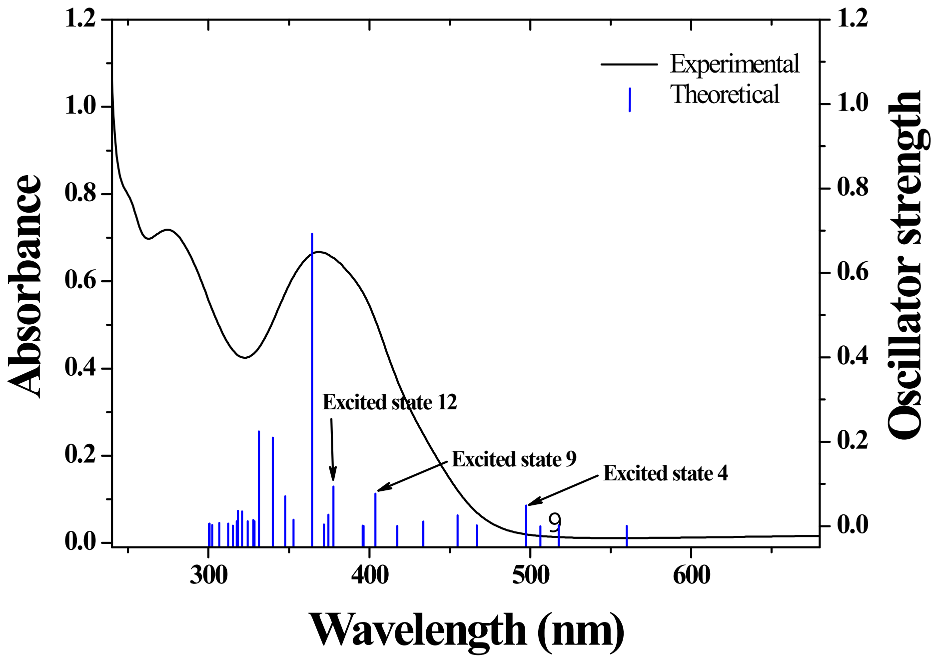

(b)

Excited State 4	Wavelength	Percent (%)	Main character	Oscillator strength
H-4 → L (β)	497.47 nm	32 %	LMCT	0.0487
H-22 → L (β)		16 %	LMCT	
H-20 → L (β)		15 %	LMCT	
H-23 → L (β)		11 %	LMCT	
H-24 → L (β)		7 %	ICT	
H-11 → L (β)		4 %	LMCT	
H-6 → L (β)		3 %	LMCT	
H-15 → L (β)		3 %	LMCT	
H-25 → L (β)		2 %	LMCT	
Excited State 9	**Wavelength**	**Percent (%)**	**Main character**	**Oscillator strength**
H-1 → L (α)	403.68 nm	39 %	ICT	0.0772
H-1 → L+1 (β)		55 %	ICT	
H-2 → L+1 (β)		3 %	ICT	
Excited State 12	**Wavelength**	**Percent (%)**	**Main character**	**Oscillator strength**
H-2 → L (α)	377.69 nm	10 %	ICT	0.0938
H-2 → L+2 (α)		8 %	ICT	
H-1 → L+1 (α)		6 %	ICT	
H-1 → L+2 (α)		6 %	ICT	
H → L+1 (α)		5 %	ICT	
H-6 → L (β)		37 %	LMCT	
H-5 → L (β)		12 %	LMCT	
H-2 → L+1 (β)		7 %	LMCT	
H-1 → L+2 (β)		6 %	MLCT	
H → L+2 (β)		3 %	ICT	
H-22 → L (β)		3 %	LMCT	
H-2 → L+3 (β)		2 %	MLCT	
H-4 → L (β)		2 %	LMCT	
H-23 → L (β)		2 %	LMCT	

Fig. S8 (a) The theoretical excitation energies and the experimental UV-vis spectrum of **1**-Cu^{2+}. (b) The major electronic transition energies and molecular orbital contributions for **1**-Cu^{2+} (H = HOMO and L = LUMO / (α): α spin MO and (β): β spin MO).

Molecular orbital (1-Cu^{2+} complex)		
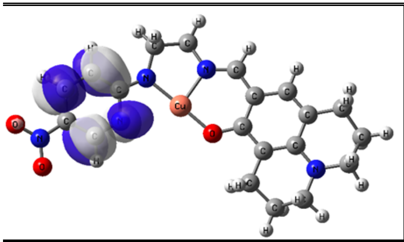	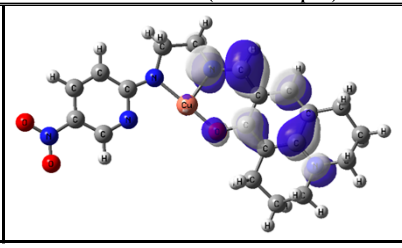	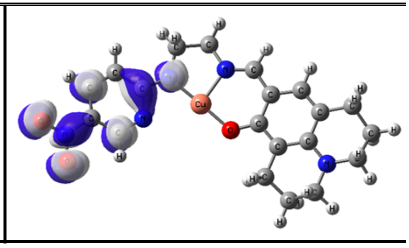
LUMO + 2 (-0.877 eV)	LUMO + 1 (-1.327 eV)	LUMO (-2.136 eV)
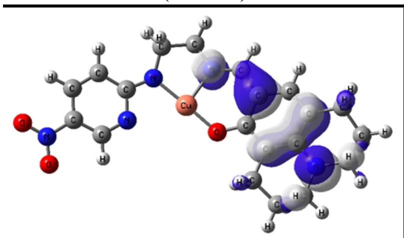	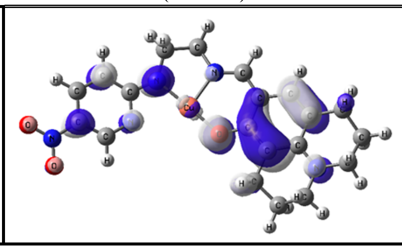	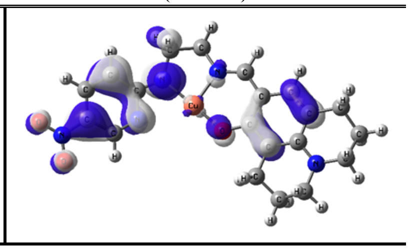
HOMO (-5.176 eV)	LUMO - 1 (-5.538 eV)	HOMO - 2 (-5.782 eV)

Fig. S9 Isosurface (0.030 electron $bohr^{-3}$) of molecular orbitals (α spin) participating in the major singlet excited states of **1**-Cu^{2+}.

Molecular orbital (1-Cu^{2+} complex)		
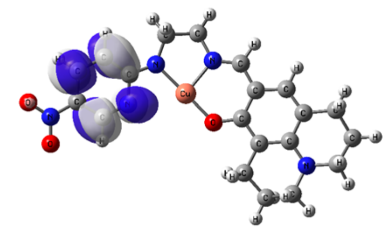	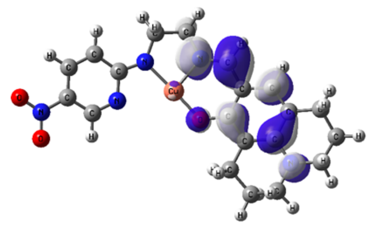	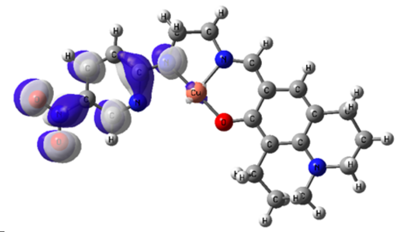
LUMO + 3 **(-0.864 eV)**	**LUMO + 2** **(-1.278 eV)**	**LUMO + 1** **(-2.109 eV)**
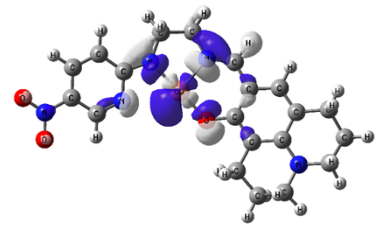	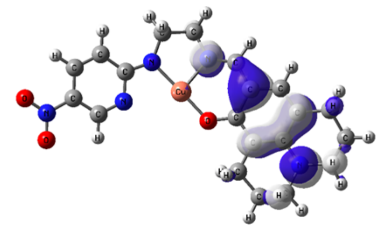	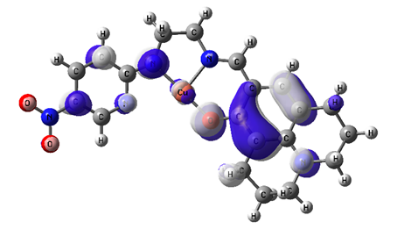
LUMO **(-3.211 eV)**	**HOMO** **(-5.147 eV)**	**HOMO - 1** **(-5.503 eV)**
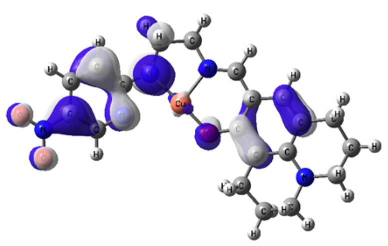	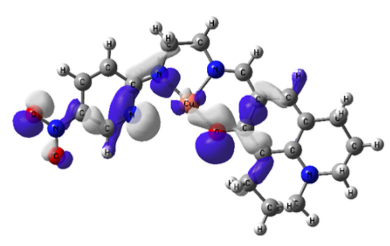	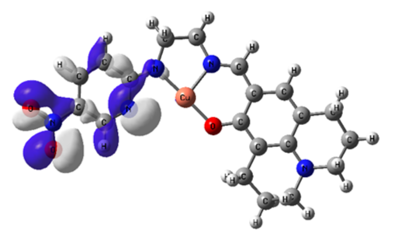
HOMO - 2 **(-5.768 eV)**	**HOMO - 4** **(-7.505 eV)**	**HOMO - 5** **(-7.678 eV)**
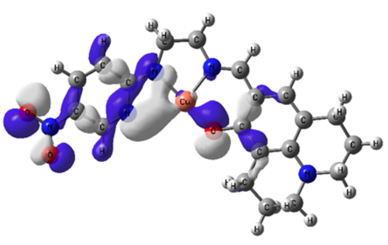	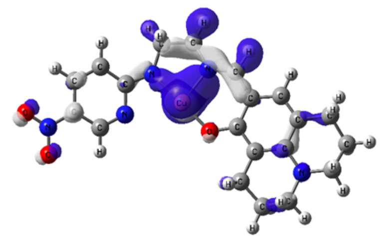	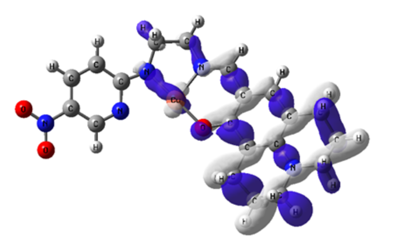
HOMO - 6 **(-7.683 eV)**	**HOMO - 11** **(-8.471 eV)**	**HOMO - 15** **(-8.902 eV)**
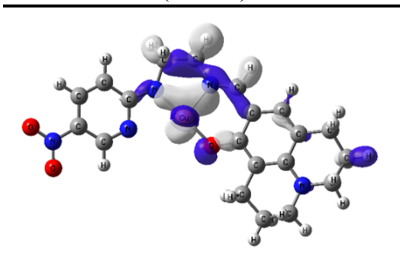	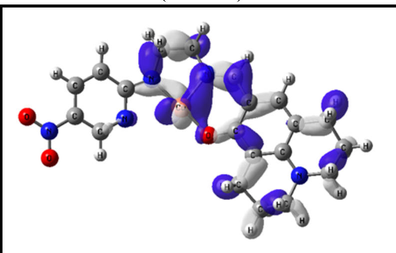	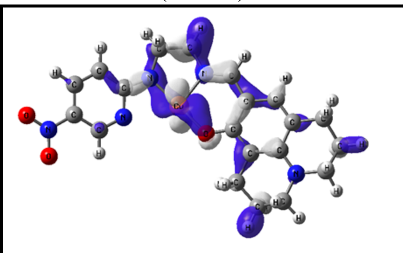
HOMO - 20 **(-9.698 eV)**	**HOMO - 22** **(-9.933 eV)**	**HOMO - 23** **(-10.071 eV)**

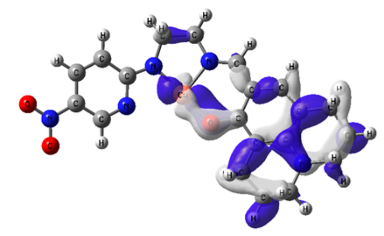	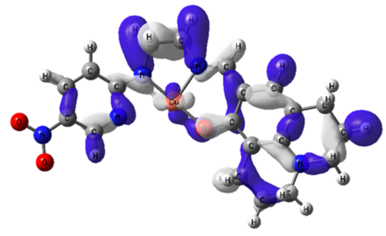
HOMO - 24 **(-10.248 eV)**	**HOMO - 25** **(-10.451 eV)**

Fig. S10 Isosurface (0.030 electron bohr^{-3}) of molecular orbitals (β spin) participating in the major singlet excited states of **1**-Cu^{2+}.

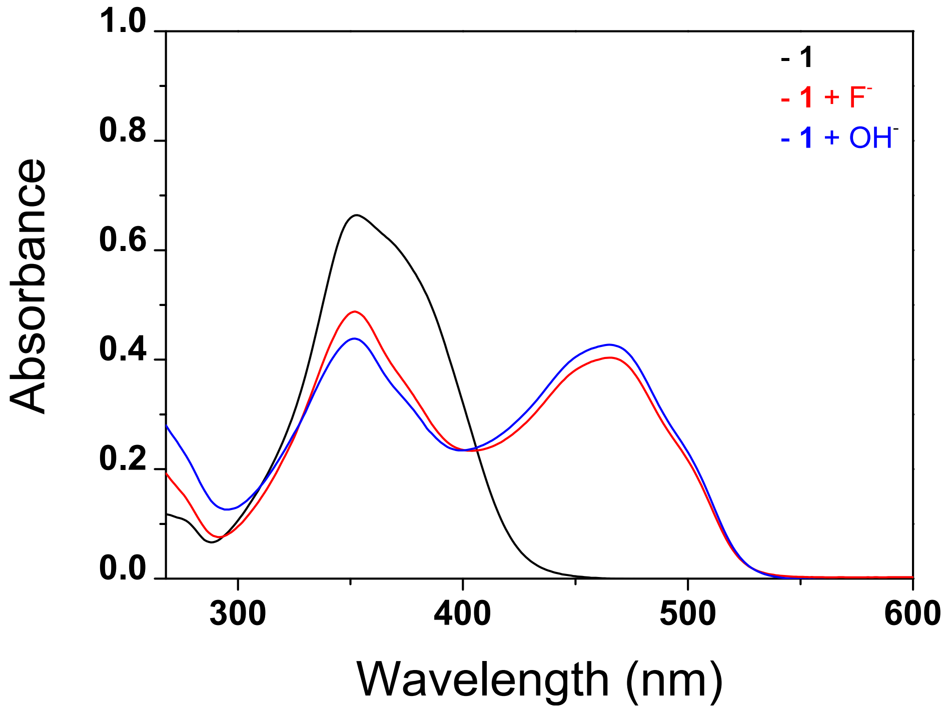

Fig. S11 Absorption changes of **1** (20 μM) in the presence of tetrabutylamonium hydroxide (20 equiv) and tetrabutylamonium fluoride (30 equiv), respectively, in DMSO.

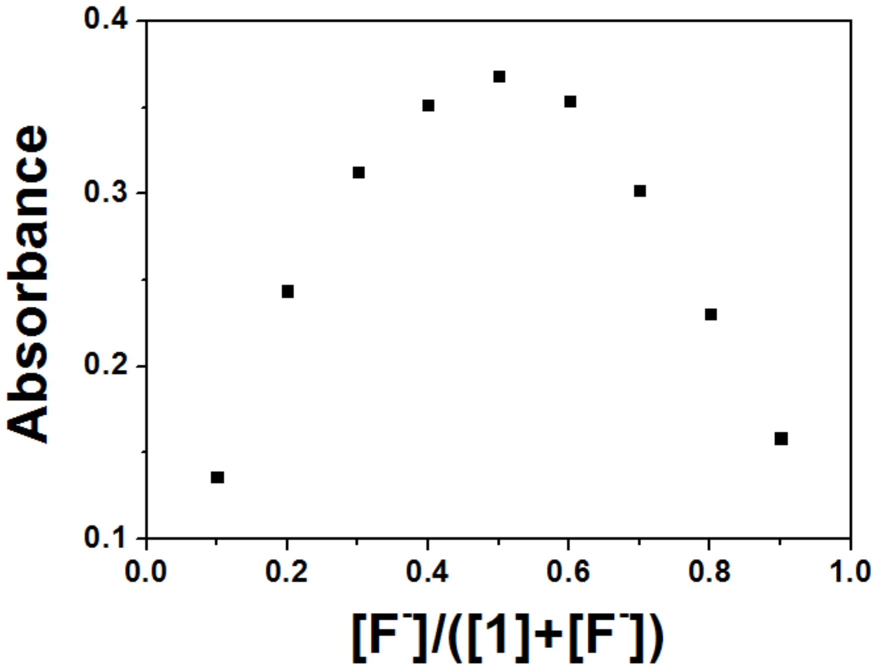

Fig. S12 Job plot of **1** and F^- in DMSO. The total concentrations of **1** and F^- were 50 μM.

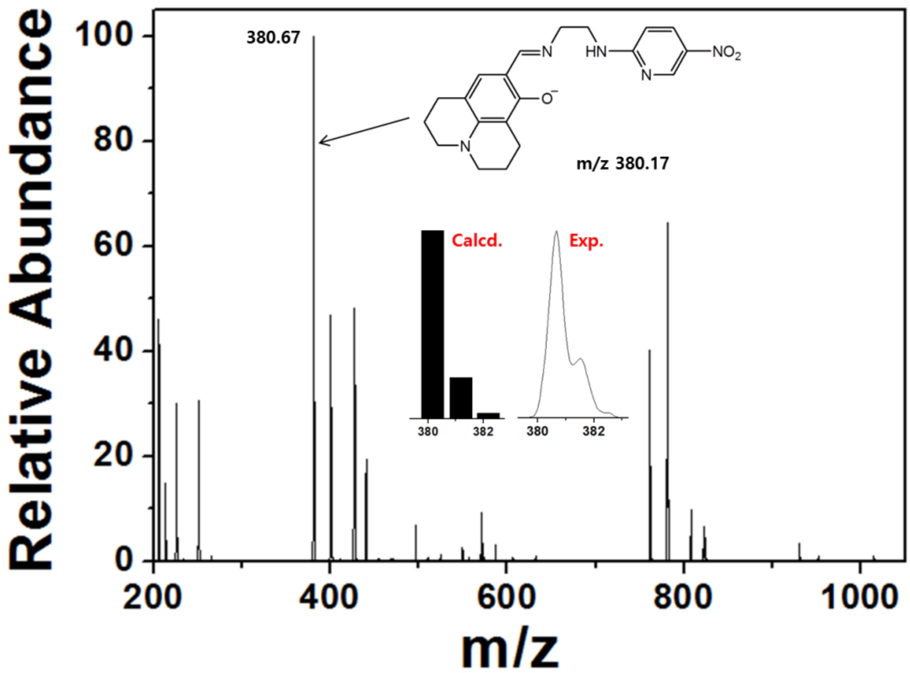

Fig. S13 Negative-ion electrospray ionization mass spectrum of **1** (100 μM) upon addition of 1 equiv of TEAF.

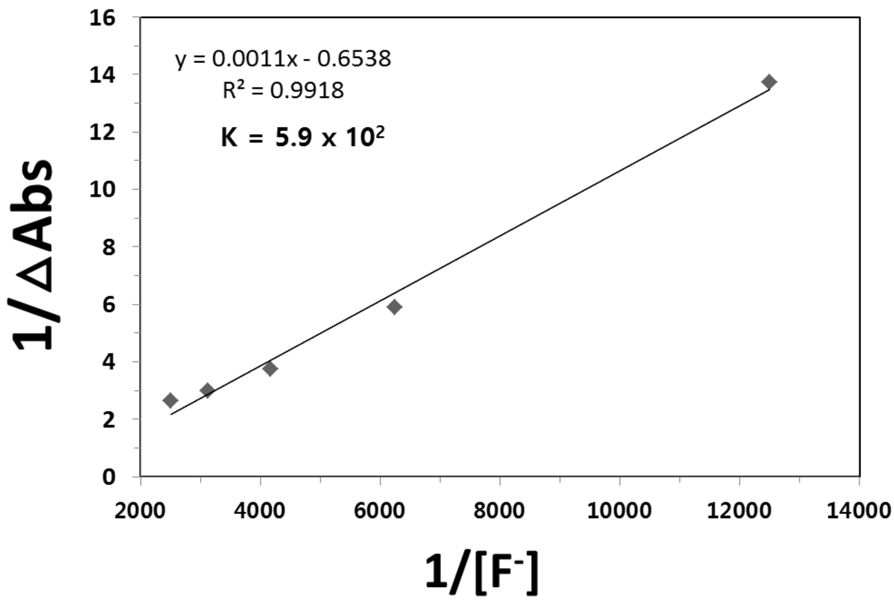

Fig. S14 Benesi-Hildebrand plot of **1** (at 465 nm), assuming 1:1 stoichiometry for association between **1** and F^-.

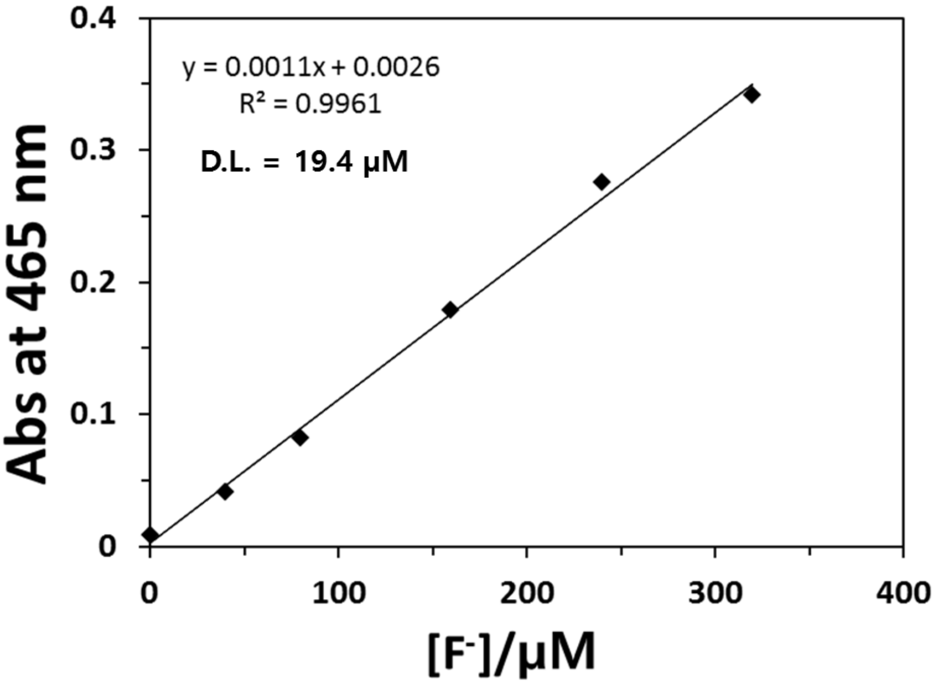

Fig. S15 Detection limit of **1** (20 μM) for F^- through change of absorbance at 465 nm.